

Properties of Cosmic Rays at energies $E > 100 \text{ TeV}$

composition resolution in air shower experiments

$$X_{\text{max}}^A = X_{\text{max}}^P - X_0 \ln A$$

$$\frac{N_e}{N_\mu} \approx 35,1 \left(\frac{E_0}{A \cdot 1 \text{ PeV}} \right)^{0,15}$$

$$\Leftrightarrow \ln\left(\frac{N_e}{N_\mu}\right) \approx C - 0,065 \ln A$$

$$\text{assume } \Delta \ln A = 1$$

$$\left. \begin{aligned} \Rightarrow \Delta X_{\text{max}} &= 37 \text{ g/cm}^2 \\ \Rightarrow \Delta \frac{N_e}{N_\mu} &= 16\% \end{aligned} \right\} \begin{array}{l} \text{realistic values} \\ \text{for modern} \\ \text{experiments} \end{array}$$

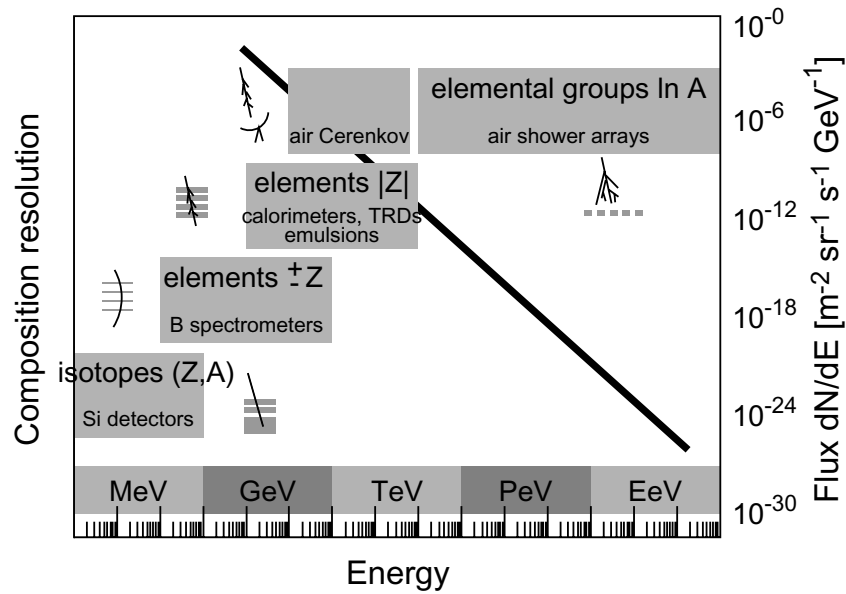


Fig. 1. Illustrative sketch of the composition resolution achieved by different cosmic-ray detection techniques as function of energy. Over the energy range shown the flux of cosmic rays decreases by about 30 orders of magnitude as indicated on the right-hand scale.

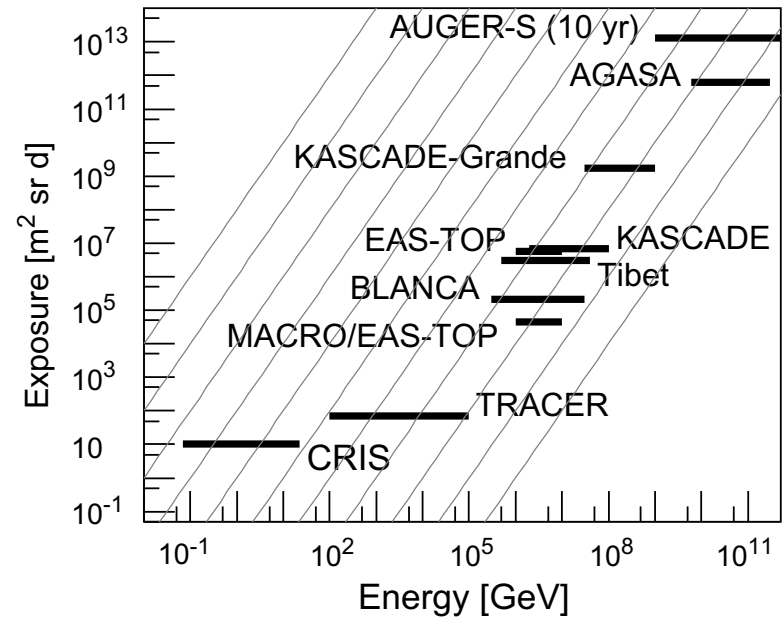


Fig. 2. Exposure of cosmic-ray experiments as function of energy for CRIS (Yanasak et al., 2001), TRACER antarctic and Sweden LDB flights (Hörandel, 2006a; Boyle, in press), MACRO/EAS-TOP (Aglietta et al., 2004b), BLANCA (Fowler et al., 2001), Tibet (Amenomori et al., 2003), EAS-TOP (Aglietta et al., 1999), KASCADE (Antoni et al., 2005), KASCADE-Grande (estimated 3 yr) (Navarra et al., 2004), AGASA, and AUGER south estimated 10 yr (Abraham et al., 2004). The grey lines are $\propto E^{-2}$.

e.g. KASCADE experiment

$$\Delta \ln A \approx 0.8$$

\Rightarrow 5 groups of elements, see below

Galactic cosmic rays and the knee in the energy spectrum

In air shower experiments detailed simulations are used to derive energy and mass of the primary particle

$(N_e, N_\mu, N_h, S_e, S_\mu, S_h, \dots, X_{max})$

$\leftarrow \rightarrow (\bar{E}, A)$
 \uparrow
simulations

The simulations describe in detail the development of the particle cascades in the atmosphere

complex calculations

- interactions of particles
- decay
- density profile of atmosphere
- B field of Earth

example of simulation code: CORSIKA

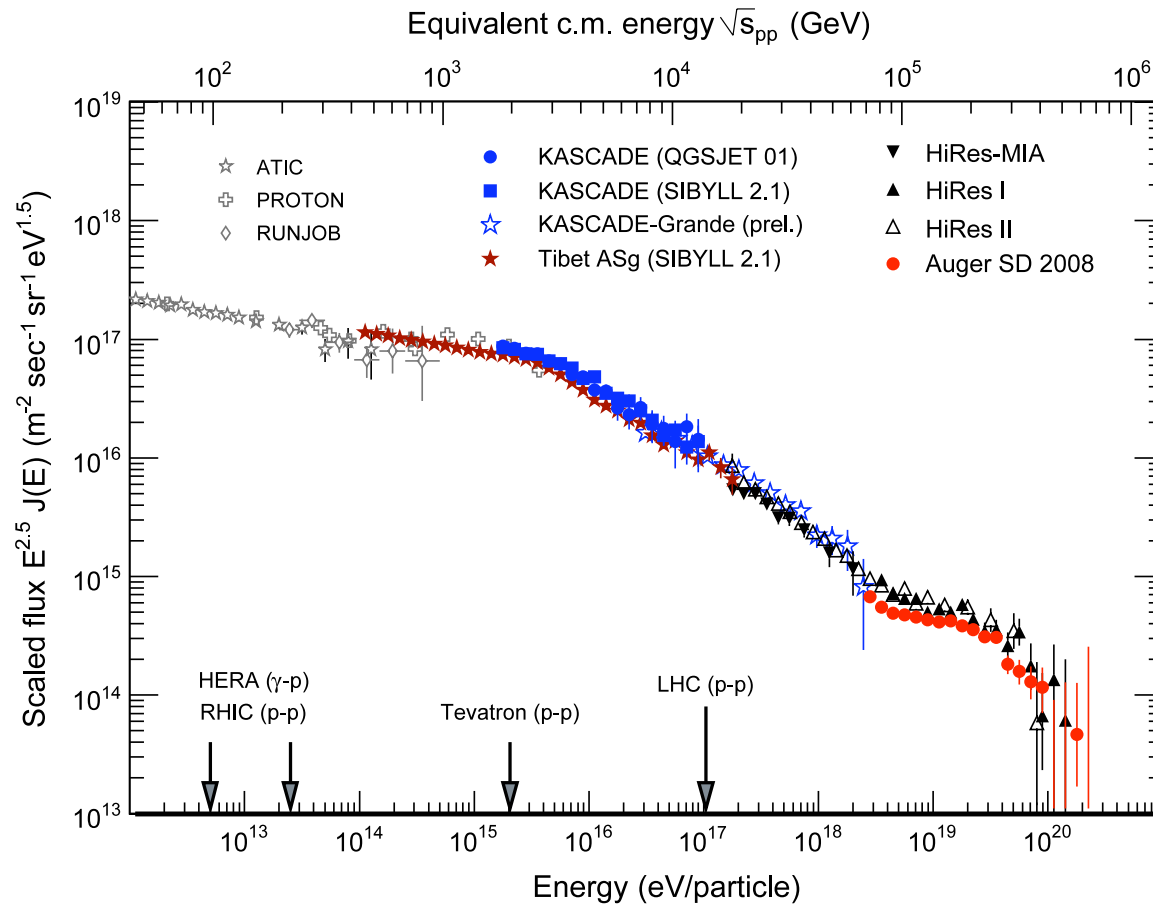
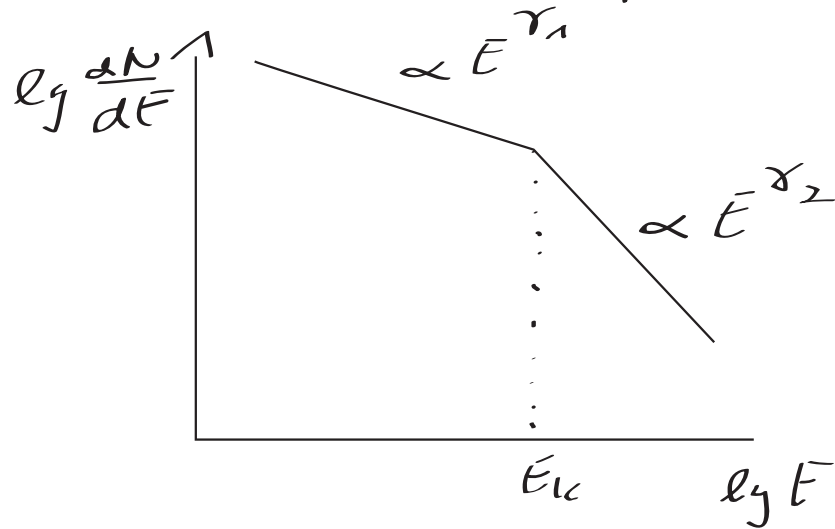


Fig. 7. All-particle cosmic-ray energy spectrum as obtained by direct measurements above the atmosphere by the ATIC [219,220], PROTON [221], and RUNJOB [222] as well as results from air shower experiments. Shown are Tibet AS γ results obtained with SIBYLL 2.1 [223], KASCADE data (interpreted with two hadronic interaction models) [224], preliminary KASCADE-Grande results [225], and Akeno data [226,33]. The measurements at high energy are represented by HiRes-MIA [227,228], HiRes I and II [229], and Auger [169].

Result: all particle energy spectrum



$$\gamma_1 \approx -2,7$$

$$\gamma_2 \approx -3,1$$

$$E_c \approx 4 \cdot 10^{15} \text{ eV}$$

all-particle spectrum is well defined

Table 3

Air shower experiments and components measured to derive the primary energy spectrum

Experiment	e	μ	h	\check{C}	F	g/cm^2	Energy shift (%)
AKENO (low energy) [73]	×	1 GeV				930	-4
BLANCA [74]	×			×		870	4
CASA-MIA [75]	×	800 MeV				870	4
DICE [76]	×	800 MeV		×		860	1
EAS-Top [77]	×	1 GeV				820	-11
HEGRA [78]	×			×		790	-10
KASCADE (electrons/muons) [79]	×	230 MeV				1022	-7
KASCADE (hadrons/muons) [80]		230 MeV	50 GeV			1022	-1
KASCADE (neural network) [81]	×	230 MeV				1022	-8
MSU [82]	×					1020	-5
Mt. Norikura [83]	×					735	9
Tibet [84]	×					606	-10
Tunka-13 [85]				×		680	0
Yakutsk (low energy) [86]				×		1020	-3
AKENO (high energy) [87]	×					930	-16
Fly's Eye [88]					×	860	-3
Gauhati [89]	×					1025	-5
Haverah Park [90]	×					1018	-10
HiRes/MIA [91]		800 MeV			×	860	-5
Yakutsk (high energy) [92]	×	1 GeV		×		1020	-20

e: Electromagnetic, μ : muonic, h: hadronic, \check{C} : Čerenkov, and F: fluorescence light. The particle thresholds are given for the muonic and hadronic components. In addition, the atmospheric overburden (g/cm^2) and the shift of the energy scale are listed.

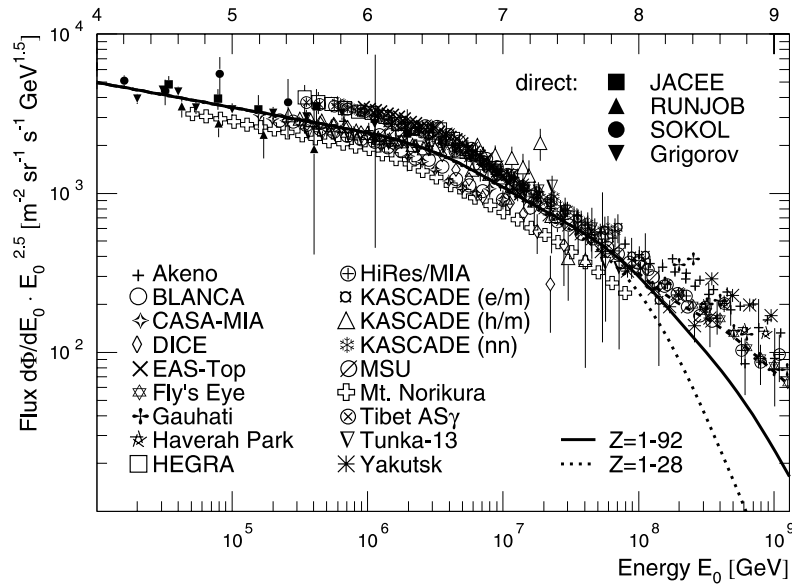


Fig. 8. All-particle energy spectra obtained from direct and indirect measurements, for references see Table 3 and text. The sum spectra for individual elements according to the poly-gonato model are represented by the dotted line for $1 \leq Z \leq 28$ and by the solid line for $1 \leq Z \leq 92$. Above 10^8 GeV the dashed line gives the normalized average spectrum.

Energy scales of individual experiments can be slightly shifted (within their systematic uncertainties). This yields a well defined all-particle energy spectrum.

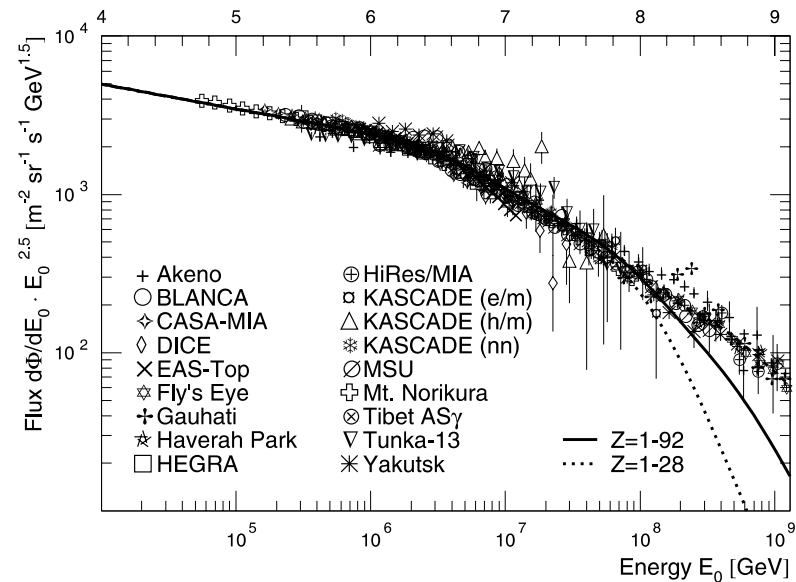
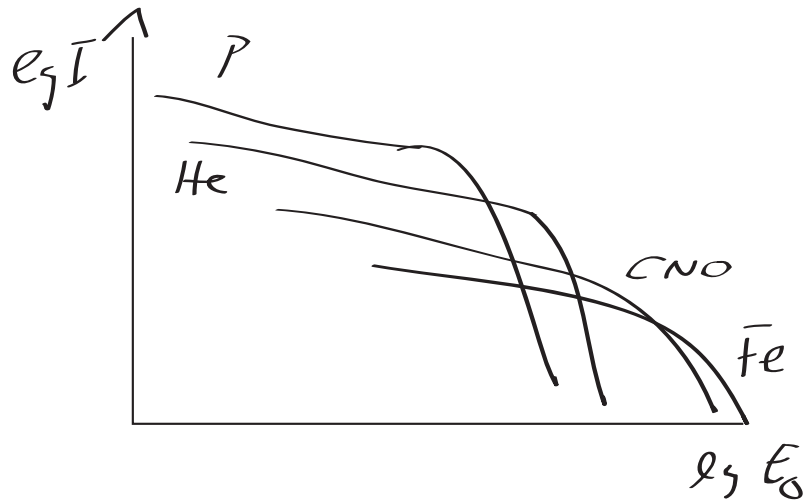


Fig. 10. Normalized all-particle energy spectra for individual experiments. The renormalization values for the energy scale and references are given in Table 3. The sum spectra for individual elements according to the poly-gonato model are represented by the dotted line for $1 \leq Z \leq 28$ and by the solid line for $1 \leq Z \leq 92$. Above 10^8 GeV the dashed line reflects the average spectrum.

Possible reasons for the knee

1) maximum energy attained during acceleration process in galactic sources

remember: $E_{\max}^{\text{SNR}} \sim Z \cdot R \cdot B \sim Z \cdot 10^{15} \text{ eV}$
 ± 1 order of magnitude



rigidity dependent
cut-off

2) Leakage from galaxy - propagation effect
extrapolation of diffusion parameters to 10^{15} eV

$$T_{esc}(E) \propto E^{\gamma} \quad \gamma = -0,6$$

$\rightarrow c T_{esc}(10^{18} \text{ eV}) \sim 300 \text{ pc}$ corresponds to
thickness of galactic disc

\rightarrow CRs cannot be magnetically bound to
the galaxy at high energies $\bar{E} > \bar{E}_k$

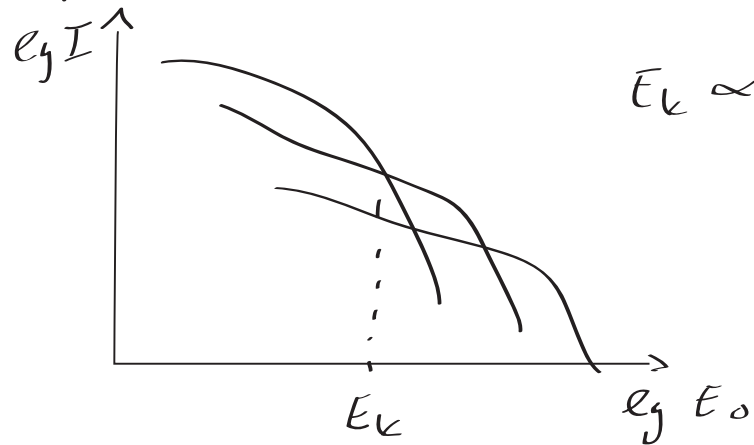
expect: same behaviour of energy spectra
as in 1) $\bar{E}_k^A \propto \bar{E}$

and anisotropy of the arrival direction
of cosmic rays
more particles from the direction of the
galactic plane

In addition to these astrophysical models also particle physics models are mentioned in the literature

- 3) Interactions with background particles
 e.g. interactions with heavy neutrinos
 from the diffuse neutrino background
 in the galaxy

spect:



$$E_k \propto A$$

cross section for interactions depends on $\frac{E}{A}$ energy per nucleon

→ mass dependent cut-off

4) new physics in the atmosphere

new interactions are postulated at high energies



↑ invisible particle (missing energy)

a fraction of the shower energy is transported into invisible channels

→ investigations of hadronic interaction models

key observables in experiments are

- all-particle spectrum

- elemental composition

 - energy spectra for groups of elements

 - mean (logarithmic) mass

- anisotropy

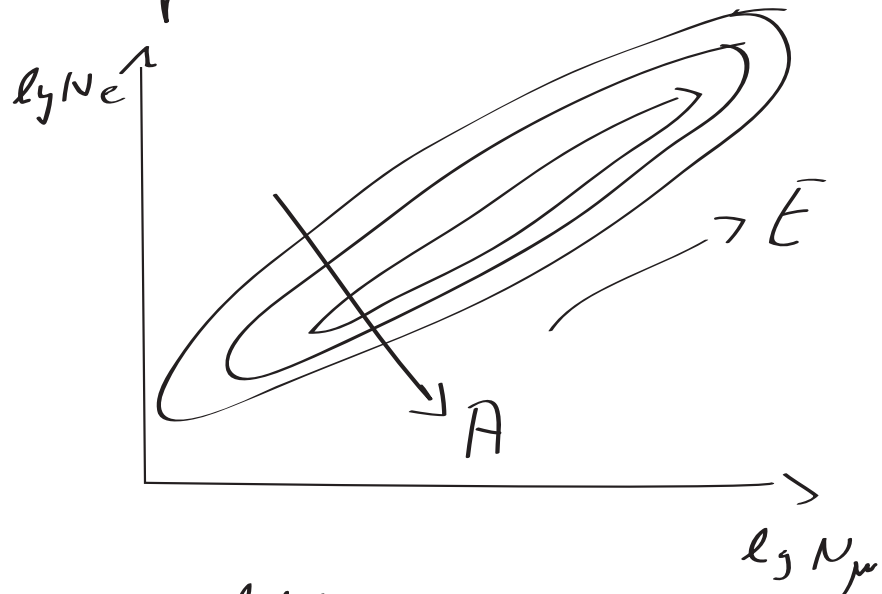
- hadronic interactions

Table 2
Synopsis of all models discussed

Model	Author(s)
<i>Source/Acceleration</i>	
Acceleration in SNR	Berezhko and Ksenofontov [18]
Acceleration in SNR + radio galaxies	Stanev et al. [19]
Acceleration by oblique shocks	Kobayakawa et al. [20]
Acceleration in variety of SNR	Sveshnikova [21]
Single source model	Erlykin and Wolfendale [22]
Reacceleration in the galactic wind	Völk and Zirakashvili [23]
Cannonball model	Plaga [24]
<i>Propagation/Leakage from Galaxy:</i>	
Minimum pathlength model	Swordy [25]
Anomalous diffusion model	Lagutin et al. [26]
Hall diffusion model	Ptuskin et al. [27], Kalmykov and Pavlov [42]
Diffusion in turbulent magnetic fields	Ogio and Kakimoto [28]
Diffusion and drift	Roulet et al [29]
<i>Interactions with background particles</i>	
Diffusion model + photo-disintegration	Tkaczyk [30]
Interaction with neutrinos in galactic halo	Dova et al. [31]
Photo-disintegration (optical and UV photons)	Candia et al. [32]
<i>New interactions in the atmosphere</i>	
Gravitons, SUSY, technicolor	Kazanas and Nicolaidis [33,34]

results of the KASCADE \bar{E} & KASCADE \bar{E} - Grande

experiments:



- > unfold energy spectra for elemental groups
- > energy spectra for groups of elements
- => elemental groups show a depression of the flux at energies $E > \bar{E}_k$
- => knee in the all-particle spectrum is caused by a cut off of the light elements

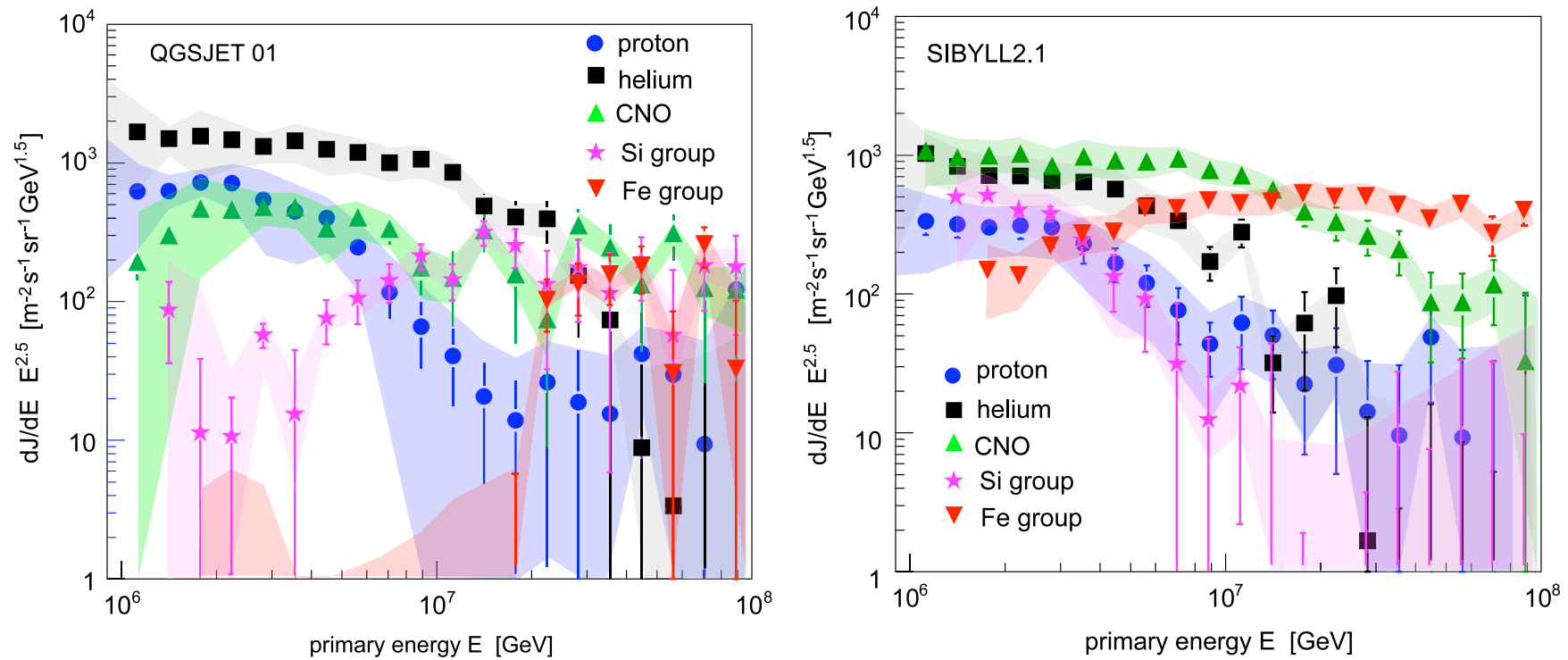
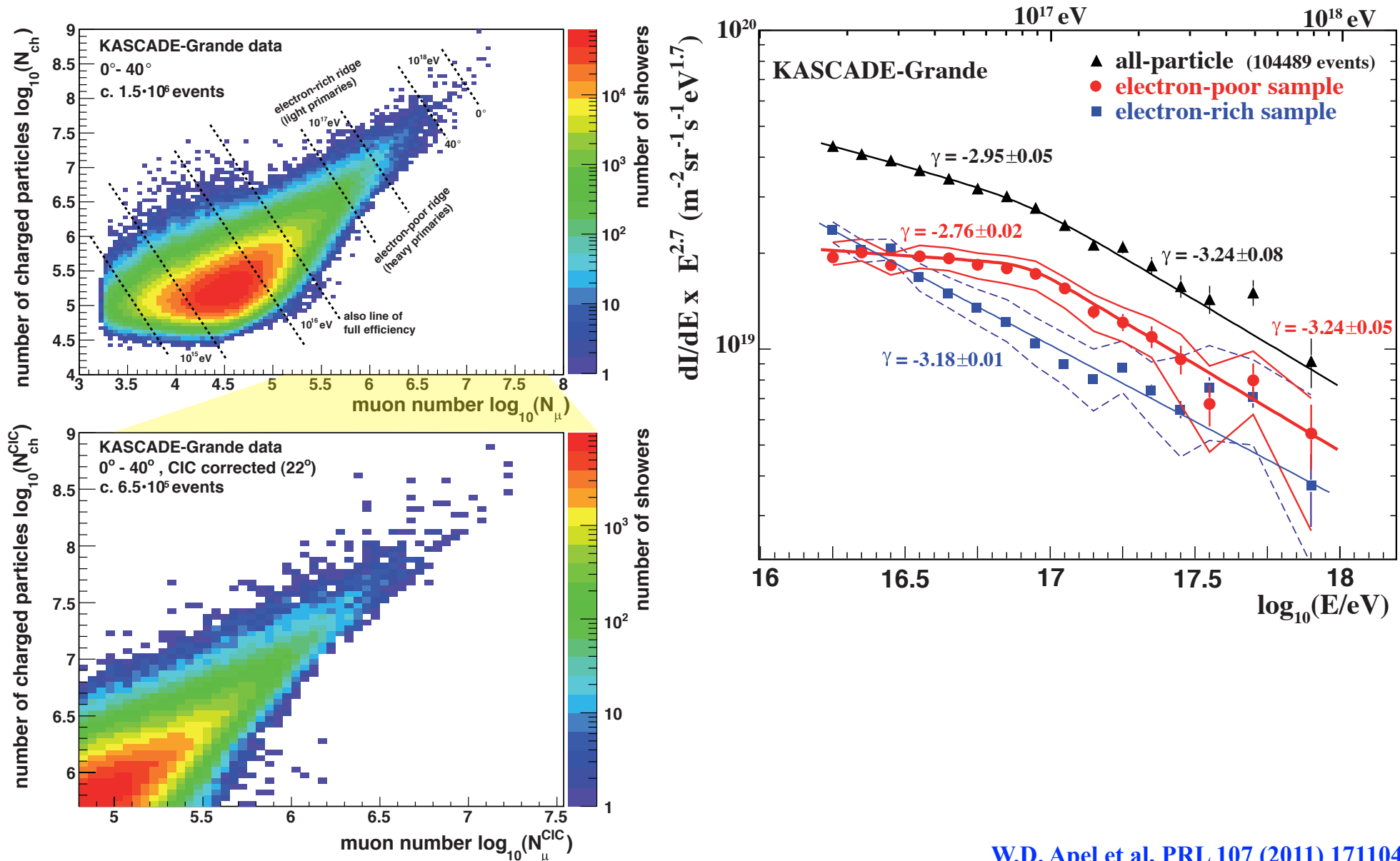


Fig. 15. Cosmic-ray energy spectrum for five groups of elements as reconstructed by the KASCADE experiment using the hadronic interaction models QGSJET 01 (left) and SIBYLL 2.1 (right) to interpret the measured data [224].

Energy spectra for groups of elements, according to KASCADE.

A knee-like structure in the spectrum of the heavy component of cosmic rays



energy spectra for individual elements/groups of elements

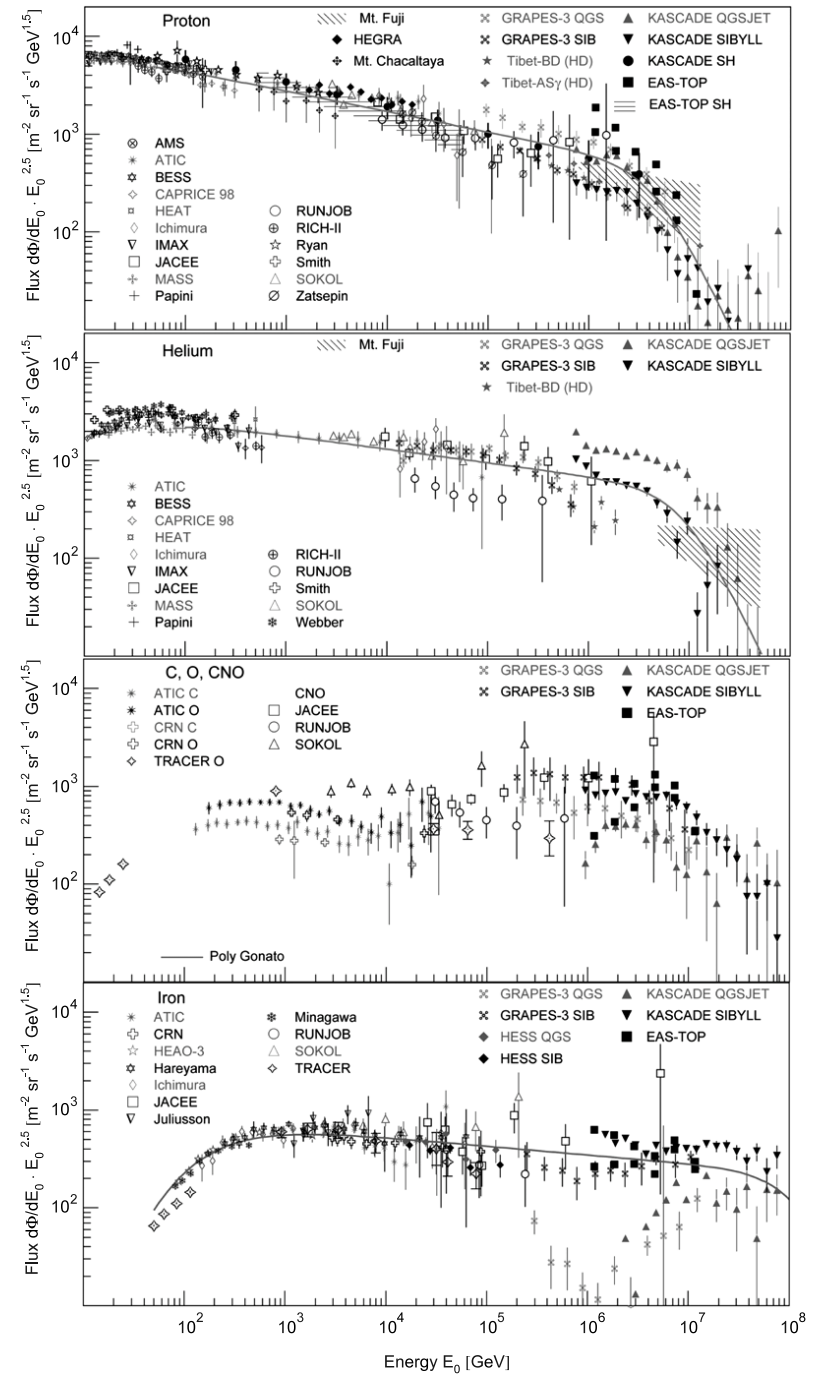


Fig. 9. Cosmic-ray energy spectra for four groups of elements, from top to bottom: protons, helium, CNO group, and iron group. **Protons:** Results from direct measurements above the atmosphere by AMS [242], ATIC [243], BESS [244], CAPRICE [245], HEAT [246,247], IMAX [248], JACEE [249], MASS [250, 251], RUNJOB [222], RICH-II [252–254], SOKOL [231,255], and fluxes obtained from indirect measurements by KASCADE electrons and muons for two hadronic interaction models [224] and single hadrons [256], EAS-TOP (electrons and muons) [257] and single hadrons [258], GRAPES-3 interpreted with two hadronic interaction models [259], HEGRA [260], Mt. Chacaltaya [261], Mts. Fuji and Kanbala [262], Tibet burst detector (HD) [263] and AS γ (HD) [264]. **Helium:** Results from direct measurements above the atmosphere by ATIC [243], BESS [244], CAPRICE [245], HEAT [246,247], IMAX [248], JACEE [249], MASS [250,251], RICH-II [252], RUNJOB [222,254], SOKOL [231,265], and fluxes obtained from indirect measurements by KASCADE electrons and muons for two hadronic interaction models [224], GRAPES-3 interpreted with two hadronic interaction models [259], Mts. Fuji and Kanbala [262], and Tibet burst detector (HD) [263]. **CNO group:** Results from direct measurements above the atmosphere by ATIC (C+O) [266], CRN (C+O) [267], TRACER (O) [268], JACEE (CNO) [269], RUNJOB (CNO) [222], SOKOL (CNO) [231], and fluxes obtained from indirect measurements by KASCADE electrons and muons [224], GRAPES-3 [259], the latter two give results for two hadronic interaction models, and EAS-TOP [257]. **Iron:** Results from direct measurements above the atmosphere by ATIC [266], CRN [267], HEAO-3 [270–272], TRACER [268] (single element resolution) and [273,247], JACEE [230], RUNJOB [222], SOKOL [231] (iron group), as well as fluxes from indirect measurements (iron group) by EAS-TOP [257], KASCADE electrons and muons [224], GRAPES-3 [259], and H.E.S.S. direct Cherenkov light [274]. The latter three experiments give results according to interpretations of the measured air-shower data with two hadronic interaction models, namely QGSJET and SIBYLL. The gray solid lines indicate spectra according to the poly-gonato model [2].

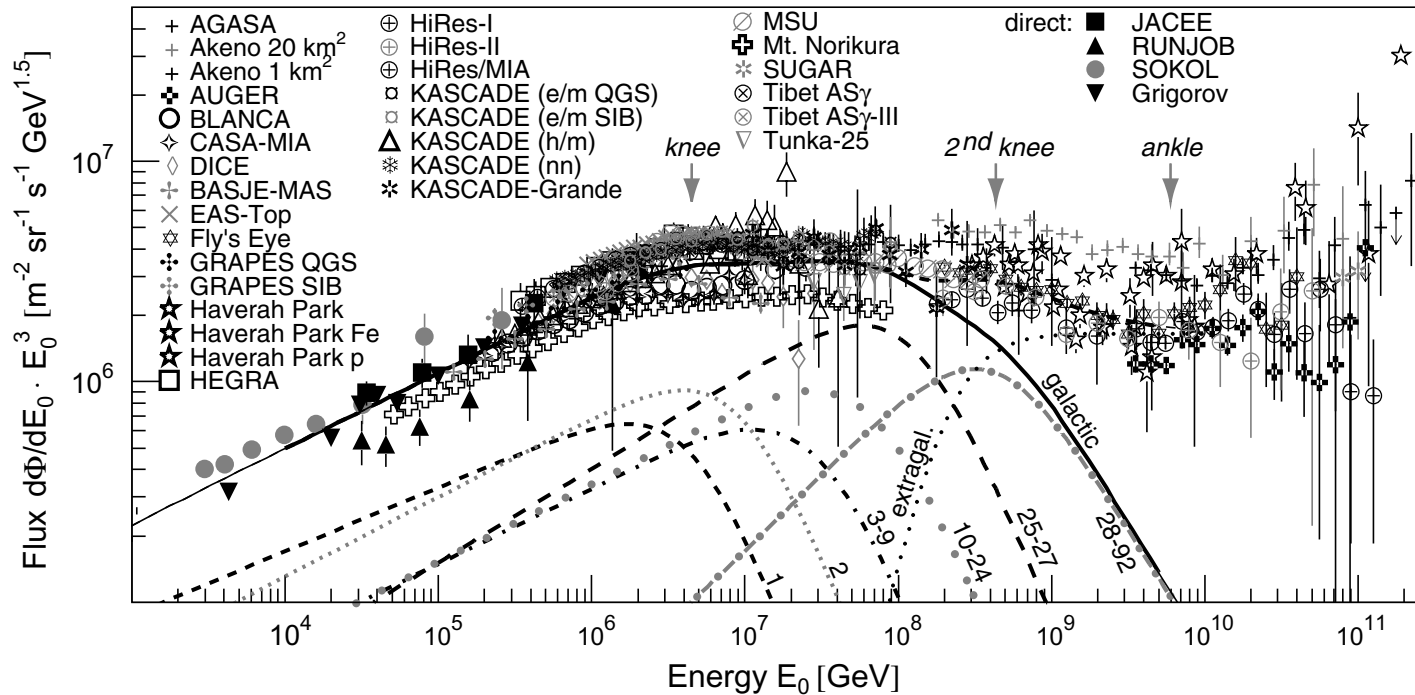


Fig. 8. All-particle energy spectrum of cosmic rays, the flux is multiplied by E^3 . Results from direct measurements by Grigorov et al. (1999), JACEE (Asakimori et al., 1995), RUNJOB (Derbina et al., 2005), and SOKOL (Ivanenko et al., 1993) as well as from the air shower experiments AGASA (Takeda et al., 2003), Akeno 1 km² (Nagano et al., 1984a), and 20 km² (Nagano et al., 1984b), AUGER (Sommers et al., 2005), BASJE-MAS (Ogio et al., 2004), BLANCA (Fowler et al., 2001), CASA-MIA (Glasmacher et al., 1999b), DICE (Swordy and Kieda, 2000), EAS-TOP (Aglietta et al., 1999), Fly’s Eye (Corbato et al., 1994), GRAPES-3 interpreted with two hadronic interaction models (Hayashi et al., 2005), Haverah Park (Lawrence et al., 1991) and (Ave et al., 2003), HEGRA (Arqueros et al., 2000), HiRes–MIA (Abu-Zayyad et al., 2001a), HiRes-I (Abbasi et al., 2004), HiRes-II (Abbasi et al., 2005), KASCADE electrons and muons interpreted with two hadronic interaction models (Antoni et al., 2005), hadrons (Hörandel et al., 1999), and a neural network analysis combining different shower components (Antoni et al., 2002), KASCADE-Grande (preliminary) (Haungs et al., in press), MSU (Fomin et al., 1991), Mt. Norikura (Ito et al., 1997), SUGAR (Anchordoqui and Goldberg, 2004), Tibet AS γ (Amenomori et al., 2000a) and AS γ -III (Amenomori et al., 2003), Tunka-25 (Chernov et al., 2006), and Yakutsk (Glushkov et al., 2003). The lines represent spectra for elemental groups (with nuclear charge numbers Z as indicated) according to the poly-gonato model (Hörandel, 2003a). The sum of all elements (galactic) and a presumably extragalactic component are shown as well. The dashed line indicates the average all-particle flux at high energies.

The all-particle flux can be described as the sum of the spectra of individual elements.

Table 2
Synopsis of all models discussed

Model	Author(s)
<i>Source/Acceleration</i>	
Acceleration in SNR	Berezhko and Ksenofontov [18]
Acceleration in SNR + radio galaxies	Stanev et al. [19]
Acceleration by oblique shocks	Kobayakawa et al. [20]
Acceleration in variety of SNR	Sveshnikova [21]
Single source model	Erlykin and Wolfendale [22]
Reacceleration in the galactic wind	Völk and Zirakashvili [23]
Cannonball model	Plaga [24]
<i>Propagation/Leakage from Galaxy:</i>	
Minimum pathlength model	Swordy [25]
Anomalous diffusion model	Lagutin et al. [26]
Hall diffusion model	Ptuskin et al. [27], Kalmykov and Pavlov [42]
Diffusion in turbulent magnetic fields	Ogio and Kakimoto [28]
Diffusion and drift	Roulet et al [29]
<i>Interactions with background particles</i>	
Diffusion model + photo-disintegration	Tkaczyk [30]
Interaction with neutrinos in galactic halo	Dova et al. [31]
Photo-disintegration (optical and UV photons)	Candia et al. [32]
<i>New interactions in the atmosphere</i>	
Gravitons, SUSY, technicolor	Kazanas and Nicolaidis [33,34]

models to explain the knee in the energy spectrum due to maximum energy achieved in accelerators

Fig. 13. Cosmic-ray energy spectra for four groups of elements, from top to bottom: protons, helium, CNO group, and iron group.

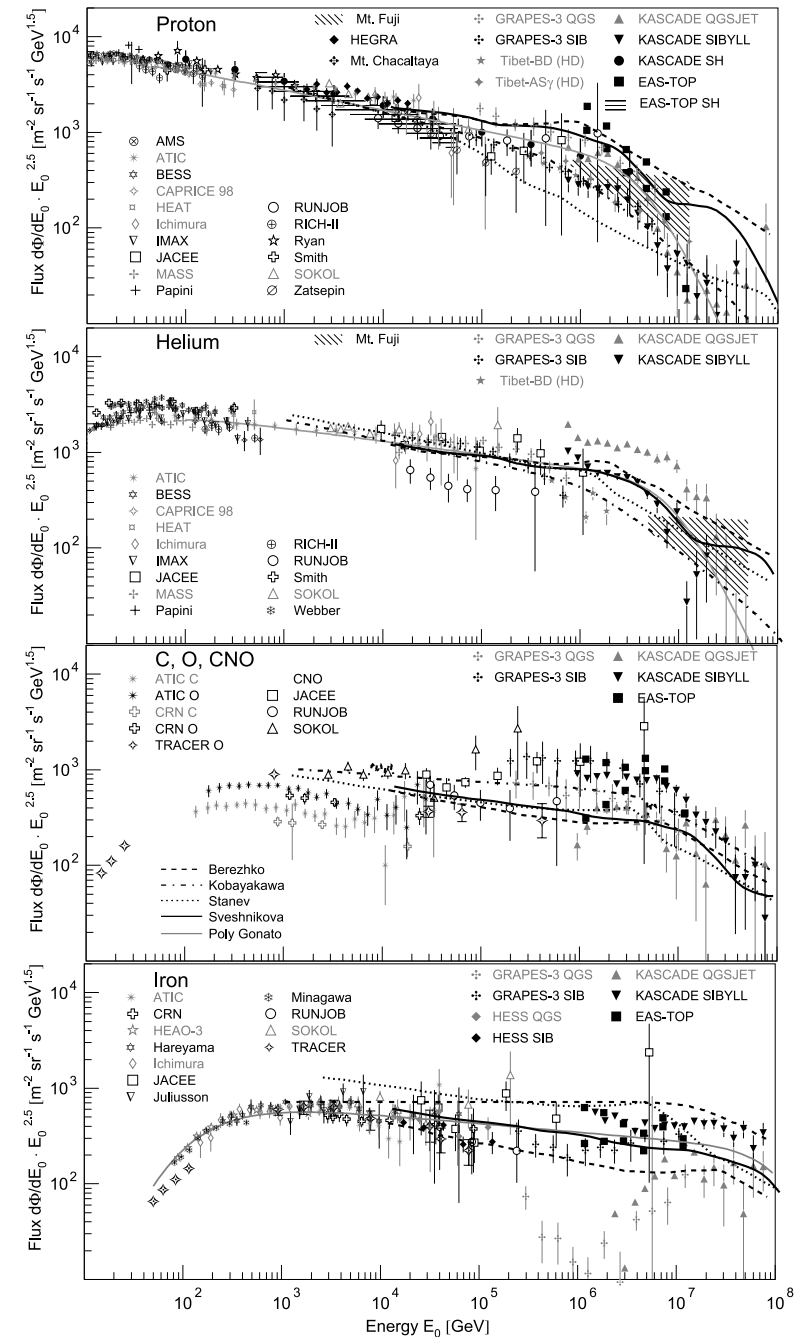
Protons: Results from direct measurements above the atmosphere by AMS (Alcaraz et al., 2000), ATIC (Wefel et al., 2005), BESS (Sanuki et al., 2000), CAPRICE (Boezio et al., 2003), HEAT (Vernois et al., 2001), Ichimura et al., 1993, IMAX (Menn et al., 2000), JACEE (Asakimori et al., 1998), MASS (Bellotti et al., 1999), Papini et al., 1993, RUNJOB (Derbina et al., 2005), RICH-II (Diehl et al., 2003), Ryan et al., 1972, Smith et al., 1973, SOKOL (Ivanenko et al., 1993), Zatsepin et al., 1993, and fluxes obtained from indirect measurements by KASCADE electrons and muons for two hadronic interaction models (Antoni et al., 2005) and single hadrons (Antoni et al., 2004b), EAS-TOP (electrons and muons) (Navarra et al., 2003) and single hadrons (Aglietta et al., 2003), GRAPES-3 interpreted with two hadronic interaction models (Hayashi et al., 2005), HEGRA (Aharonian et al., 1999), Mt. Chacaltaya (Inoue et al., 1997), Mts. Fuji and Kanbala (Huang et al., 2003), Tibet burst detector (HD) (Amenomori et al., 2000b) and AS γ (HD) (Amenomori et al., 2004).

Helium: Results from direct measurements above the atmosphere by ATIC (Wefel et al., 2005), BESS (Sanuki et al., 2000), CAPRICE (Boezio et al., 2003), HEAT (Vernois et al., 2001), Ichimura et al. (1993), IMAX (Menn et al., 2000), JACEE (Asakimori et al., 1998), MASS (Bellotti et al., 1999), Papini et al. (1993), RICH-II (Diehl et al., 2003), RUNJOB (Derbina et al., 2005), Smith et al. (1973), SOKOL (Ivanenko et al., 1993), Webber et al. (1987), and fluxes obtained from indirect measurements by KASCADE electrons and muons for two hadronic interaction models (Antoni et al., 2005), GRAPES-3 interpreted with two hadronic interaction models (Hayashi et al., 2005), Mts. Fuji and Kanbala (Huang et al., 2003), and Tibet burst detector (HD) (Amenomori et al., 2000b).

CNO group: Results from direct measurements above the atmosphere by ATIC (C + O) (Cherry, 2006), CRN (C + O) (Müller et al., 1991), TRACER (O) (Müller et al., 2005), JACEE (CNO) (JACEE collaboration, 1999), RUNJOB (CNO) (Derbina et al., 2005), SOKOL (CNO) (Ivanenko et al., 1993), and fluxes obtained from indirect measurements by KASCADE electrons and muons (Antoni et al., 2005), GRAPES-3 (Hayashi et al., 2005), the latter two give results for two hadronic interaction models, and EAS-TOP (Navarra et al., 2003).

Iron: Results from direct measurements above the atmosphere by ATIC (Cherry, 2006), CRN (Müller et al., 1991), HEAO-3 (Engelmann et al., 1985), Juliusson (1974), Minagawa (1981), TRACER (Müller et al., 2005) (single-element resolution) and Hareyama et al. (1999), Ichimura et al. (1993), JACEE (Asakimori et al., 1995), RUNJOB (Derbina et al., 2005), SOKOL (Ivanenko et al., 1993) (iron group), as well as fluxes from indirect measurements (iron group) by EAS-TOP (Navarra et al., 2003), KASCADE electrons and muons (Antoni et al., 2005), GRAPES-3 (Hayashi et al., 2005), and HESS direct Čerenkov light (Aharonian et al., 2007). The latter three experiments give results according to interpretations with two hadronic interaction models.

Models: The grey solid lines indicate spectra according to the poly-gonato model (Hörandel, 2003a). The black lines indicate spectra for models explaining the knee due to the maximum energy attained during the acceleration process according to Sveshnikova (2003) (—), Berezhko and Ksenofontov (1999) (- - -), Stanev et al. (1993) (· · ·), and Kobayakawa et al. (2002) (- · -).



models to explain the knee in the energy spectrum due to leakage from Galaxy

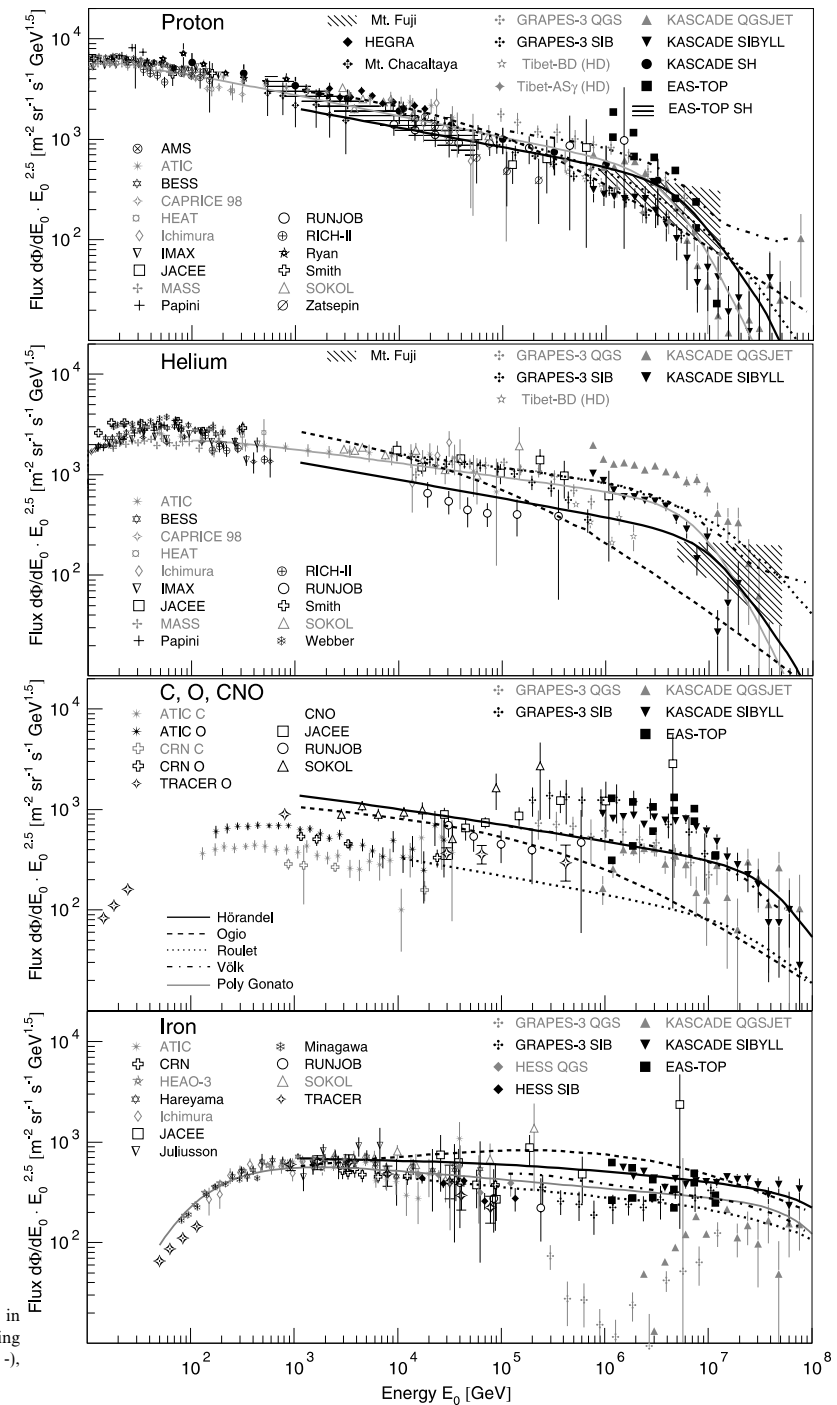


Fig. 14. Cosmic-ray energy spectra for four groups of elements, from top to bottom: protons, helium, CNO group, and iron group. (Refer to note in Fig. 13.) The grey solid lines indicate spectra according to the poly-gonato model (Hörandel, 2003a). The black lines indicate spectra for models explaining the knee as effect of leakage from the Galaxy during the propagation process according to Hörandel et al. (2007) (—), Ogio and Kakimoto (2003) (- - -), Roulet (2004) (· · ·), as well as Völk and Zirakashvili (2003) (- · - ·).

- compilation of world data set for the energy spectra for groups of elements exhibiting a cut-off compatible with $E_k \propto t$
- all-particle energy spectrum can be described as sum of the spectra for individual elements with $E_k \propto t$
- a detailed comparison of the predictions of models to explain the knee with experimental data indicates:
 - data are compatible with scenarios 1) & 2) above, i.e. maximum energy attained in SNR and leakage from Galaxy